ACS APPLIED MATERIALS & INTERFACES

RESEARCH ARTICLE

www.acsami.org

Near-Infrared Azadipyrromethenes as Electron Donor for Efficient Planar Heterojunction Organic Solar Cells

Sibel Y. Leblebici, Luis Catane, David E. Barclay, Tara Olson, Teresa L. Chen, and Biwu Ma*

The Molecular Foundry, Lawrence Berkeley National Laboratory, Berkeley, California 94720, United States

Supporting Information

ABSTRACT: We report the use of three solution processable azadipyrromethene (ADPM) based compounds, i.e., ADPM, B,F_2-chelated ADPM (BF2-ADPM), and B,O-chelated ADPM (BO-ADPM), as electron donors in planar heterojunction solar cells. These small molecules possess exceptional light harvesting capability with high extinction coefficients ($\sim 1 \times 10^5$ M^{-1} cm^{-1} in solutions) and broad absorption spectra up into the near-infrared region. Planar heterojunction organic solar cells, consisting of a solution processed electron donor layer and a vapor deposited C_{60} acceptor layer, have been constructed to give power conversion efficiencies of 0.56, 0.69, and 2.63% for ADPM, BF2-ADPM, and BO-ADPM, respectively, under AM 1.5G simulated 1 sun solar illumination. A high open circuit voltage (V_{oc}) of ~0.8 V was achieved for the BO-ADPM/C_{60} device, which is among the highest reported values for organic solar cells with photocurrent generation in the near-infrared region beyond 1.5 eV.

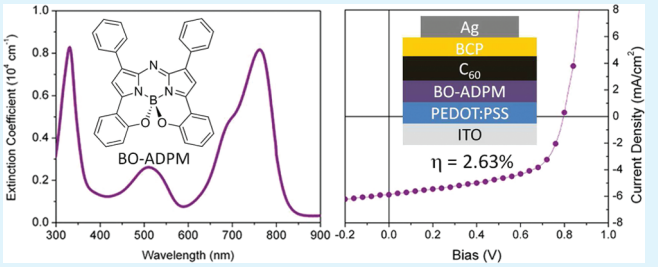

KEYWORDS: organic solar cells, near-infrared dyes, azadipyrromethenes, solution processable, planar heterojunction

INTRODUCTION

Organic semiconductors provide an inexpensive pathway to fabricating thin and lightweight new generation solar energy conversion devices. The tunability of organic molecular structures enables a variety of low-cost organic semiconductors to be developed for use in electronic devices.[1,2] To date, three main categories of organic semiconductors have been extensively investigated for organic solar cells (OSCs), including solution processable conjugated polymers, vapor depositable small molecules, and solution-processable small molecules. In recent years, solution processable small molecules have attracted great attention due to their numerous advantages over the other two classes of materials, i.e., higher purity, more reproducible and scalable synthesis, and higher stability over polymers, as well as allowing higher throughput device manufacturing via solution processing instead of high vacuum conditions for vapor-deposited small molecule devices.[3,4] The power conversion efficiencies of organic solar cells based on solution processable small molecules have steadily improved over the past few years from ~1 to more than 5%, catching up to those of polymer and vapor deposited small molecule devices.[5,6]

The efficiency of a typical photovoltaic cell depends on the short-circuit current density (J_{sc}), the open circuit voltage (V_{oc}) and the fill factor (FF). Because the light-harvesting capability of the organic layers represents one of the major factors in determining the J_{sc}, low bandgap materials with high absorption coefficients and strong spectral overlap with solar irradiation are desired.[3] For this reason, a variety of near-infrared organic dyes have been explored over the past few years for OSCs, including phthalocyanines,[7−9] subphthalocyanines,[10] merocyanines,[11] squaraine,[12] isoindigos,[13,14] borondipyrromethenes,[15] and diketopyrrolopyrroles.[16] On the other hand, the V_{oc} is generally considered to be controlled by the energy offset (ΔE_{DA}) between the highest occupied molecular orbital (HOMO) of the donor and the lowest unoccupied molecular orbital (LUMO) of the acceptor,[17] as well as the morphological properties of the donor/acceptor interface.[18] It is not trivial to maintain a high V_{oc} for solar cells with near-infrared materials, or to achieve high J_{sc} and V_{oc} simultaneously, as the reduced bandgap of electron donors often results in lower ΔE_{DA}.

Herein, we report for the first time a series of solution-processable azadipyrromethene based small molecules, i.e., azadipyrromethene (ADPM), B,F_2-chelated azadipyrromethene (BF2-ADPM), and B,O-chelated azadipyrromethene (BO-ADPM), being used in OSCs. Because of their facile synthesis, high solubility, high stability, and exceptional photophysical properties with high absorption coefficients ($\sim 1 \times 10^5$ M^{-1} cm^{-1}) and fluorescence quantum yields in the near-infrared region,[19−21] ADPM based organic dyes have previously been exploited in a diverse range of material and biological applications, such as photosensitizers for photodynamic therapy,[22,23] fluorescent probes for biological imaging[24,25] and as laser dyes.[26] By using

Received: August 26, 2011
Accepted: October 15, 2011
Published: October 16, 2011

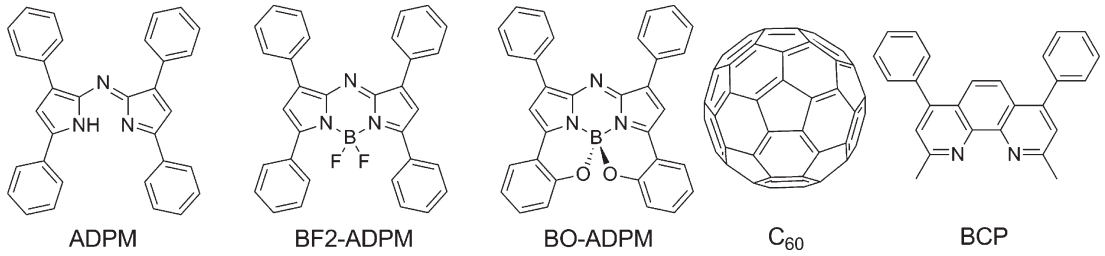

Figure 1. Chemical structures of the materials used in this study.

these near-infrared dyes as electron donors and C_{60} as the acceptor, we have constructed efficient planar heterojunction OSCs. Of particular interest is the BO-ADPM/C_{60} bilayer device exhibiting power conversion efficiencies up to 2.63%, which is attributed to the photocurrent generation into the near-infrared spectrum of up to 845 nm while maintaining high V_{oc} of ~0.8 V.

EXPERIMENTAL SECTION

Materials and Instrumentation. The three ADPM compounds, shown in Figure 1, were synthesized following the procedures reported in the literature.[22,24] More information regarding the materials synthesis and characterizations can be found in the Supporting Information.

Prepatterned ITO-coated glass substrates were purchased from Thin Film Devices Inc. Sublimed grade C_{60} and Bathocuproine (BCP) were purchased from Aldrich. PEDOT:PSS (Baytron PH 500) was purchased from H. C. Starck. UV−vis measurements of materials in solution and in film form were conducted with a CARY 5000 UV−vis−NIR spectrophotometer. Film thickness was measured using a Dektak 150 profilometer. Cyclic voltammetry was performed using a Solartron 1285 potentiostat, wherein a platinum wire acts as the working and counter electrode and a silver wire as the reference electrode. Samples were prepared in dichloromethane solution with 0.1 M tetrabutylammonium hexafluorophosphate as the electrolyte at a scan rate of 100 mV s^{-1}. Atomic force microscopy (AFM) images were taken on a Veeco Nanoscope V scanning probe microscope in tapping-mode. A Thermal-Oriel 300W solar simulator provided an AM 1.5G solar illumination at 100 mW cm^{-2} for device testing. A Keithley 236 source-measure unit was used to measure current density−voltage (*J-V*) curves. External quantum efficiencies (EQEs) were measured with a monochromator and calibrated up to 800 nm with a silicon photodiode.

Device Fabrication. Organic solar cells were fabricated in a planar heterojunction structure of ITO/PEDOT:PSS/ADPM donor/C_{60}/BCP/Ag. ITO-coated glass substrates were cleaned by successive sonication in soap solution, deionized water, acetone and isopropanol for 15 min at 40 °C and UV ozone cleaned for 10 min. An ~40 nm thick PEDOT:PSS layer was prepared by spin-casting its aqueous solution onto the cleaned ITO-coated glass substrate at 4000 rpm for 40 s and baked at 140 °C for 20 min. ADPM, BF2-ADPM, and BO-ADPM were dissolved in chlorobenzene at a concentration of 4 mg/mL. Additionally, BO-ADPM was dissolved in tetrahydrofuran (THF) at 2 mg/mL. All solutions were passed through a 0.2 μm polytetrafluorethylene filter prior to being spin-coated onto the PEDOT:PSS film at 2000 rpm for 60 s. Subsequently, the C_{60} (45 nm), BCP (10 nm), and Ag (100 nm) were thermally evaporated under high vacuum (~ 2×10^{-6} mbar) at rates of 1.5, 1.5, and 4 Å s^{-1}, respectively. The BCP layer acts to block excitons and transport electrons.[5] The Ag electrodes defined the devices with a shadow mask of 0.03 cm^2 in area. Hole-only devices were fabricated with the structure of ITO/PEDOT:PSS/ADPM donor/Au. The hole-only devices were used to study hole mobility via the space-charge limited current (SCLC) method.

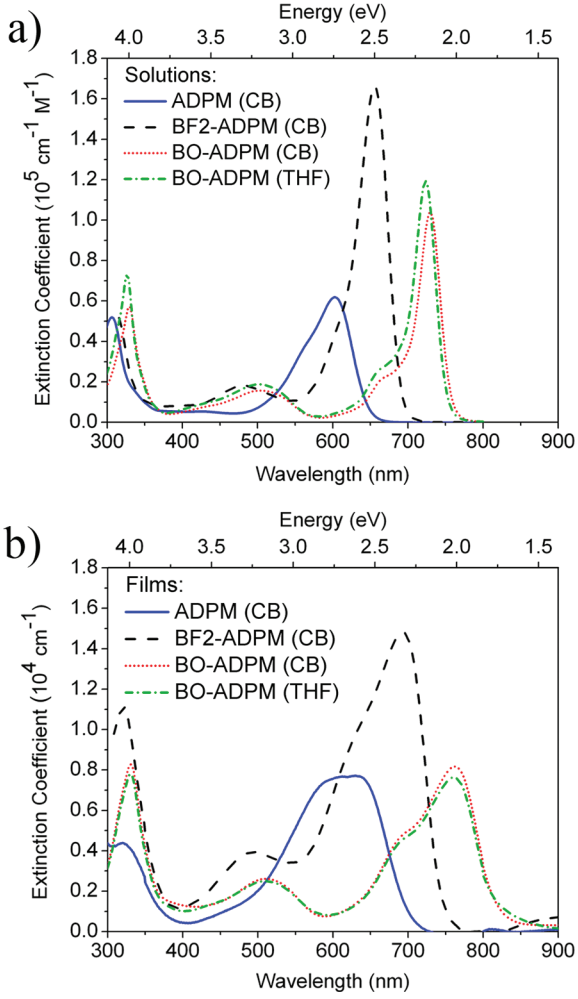

Figure 2. Extinction coefficients of ADPM, BF2-ADPM, and BO-ADPM in (a) solutions and (b) thin films that involved the cholorbenzene (CB) and THF solvents. The extinction coefficients in the thin films are ~10× smaller than in solution.

RESULTS AND DISCUSSION

Physical Properties. The solution UV−vis absorption spectra were recorded in cholorbenzene for all three molecules and also in THF for BO-ADPM (Figure 2a). Their corresponding thin film absorption spectra are shown in Figure 2b, which were measured on ITO/PEDOT:PSS coated glass substrates. We found that all three ADPM molecules display extremely high extinction coefficients, reaching up to ~1.7×10^5 M^{-1} cm^{-1} in solution and ~1.5×10^4 cm^{-1} in thin film. Also, significant

broadening and a bathochromic shift of the absorption peaks in the thin film were observed, which is considered to be the result of strong molecular $\pi-\pi$ interactions due to the flat molecule structures. The red shift of the absorption spectra from ADPM to BF2-ADPM and BO-ADPM is attributed to the electron-withdrawing nature of the B,F_2[27] and B,O chelates, as well as the intramolecular B−O ring formation.[24] It is worth highlighting that BO-ADPM absorbs in the near-infrared region up to ~800 nm in solution and ~850 nm in the thin film regardless of the solvent used. The optical bandgaps for the three materials were determined from the onset of the thin film absorption spectra, which are 1.70 eV for ADPM, 1.59 eV for BF2-ADPM, and 1.47 eV for BO-ADPM.

Cyclic voltammetry was used to investigate the electrochemical properties of this family of molecules. The cyclic voltammetry curves for the three molecules are available in the Supporting Information. The oxidation and reduction potentials relative to an internal ferrocene/ferrocenium redox couple (−4.8 eV vs vacuum) translates into reductions in electrochemical bandgaps of 1.88, 1.74, and 1.46 eV for ADPM, BF2-ADPM, and BO-ADPM, respectively. The trend observed in the electrochemical bandgap values for the three compounds corresponds well to that for the optical bandgaps.

The HOMO and LUMO levels were estimated to be −5.38 and −3.50 eV for ADPM, − 5.68 and −3.94 eV for BF2-ADPM, and −5.48 and −4.02 eV for BO-ADPM, respectively. The resulting energy level diagram is shown in Figure 3. Density Functional Theory calculations predicted quite consistent results for the changes in energy levels and bandgaps (see the Supporting Information). The HOMO and LUMO levels of these molecules suggest their suitable application as electron donors in OSCs with C_{60} as the acceptor, which has a HOMO of −6.2 and a LUMO of −4.5 eV.[5]

The hole carrier mobility of the ADPM films was evaluated by SCLC measurements. The SCLC hole-only devices were fabricated with the structure of ITO/PEDOT:PSS/ADPM film/Au, wherein the ADPM films were prepared by spin-casting chloroform solutions of ADPM and BF2-ADPM, and cholorbenzene and THF solutions of BO-ADPM. Chloroform was used for ADPM and BF2-ADPM to ensure sufficiently thick films needed for SCLC measurements (>100 nm). The resulting SCLC hole mobility values are shown in Table 1. Thin films of ADPM and BF2-ADPM prepared from chloroform solutions, and BO-ADPM from cholorbenzene solution exhibit very similar mobility values of $1-2 \times 10^{-4}$ $cm^2\ V^{-1}s^{-1}$. While a lower hole mobility of 2.88×10^{-5} $cm^2\ V^{-1}s^{-1}$ was obtained for BO-ADPM thin films processed in THF. This difference in hole mobility indicates distinct film morphologies for the films prepared via various solvents. It is very likely that the BO-ADPM film from THF is amorphous and the film from cholorbenzene has more crystalline features.[18]

The surface morphology of the thin films was studied with tapping mode AFM. Thin films were prepared via spin-casting of cholorbenzene solutions of all three compounds with an additional BO-ADPM film prepared from THF. The AFM images of the four films are shown in Figure 4. The BF2-ADPM and both BO-ADPM films exhibit uniform and smooth morphologies

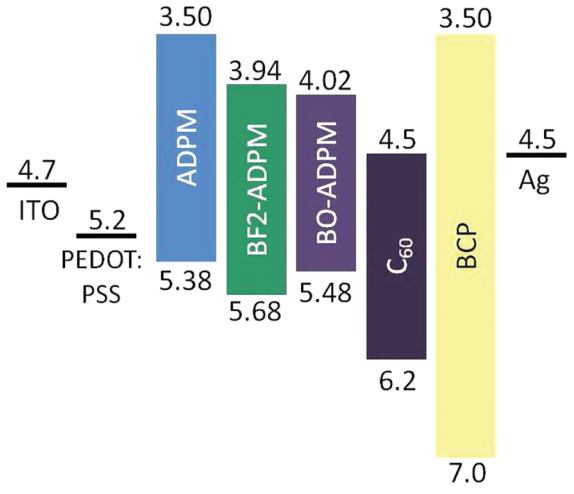

Figure 3. Schematic energy levels in eV of organic thin films and electrodes.

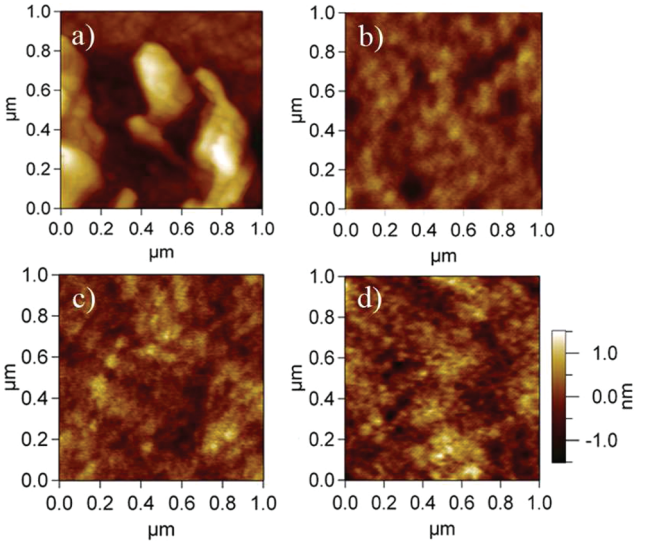

Figure 4. Tapping mode AFM images of spin-cast films of (a) ADPM from chlorobenzene, (b) BF2-ADPM from chlorobenzene, (c) BO-ADPM from chlorobenzene, and (d) BO-ADPM from THF. The height scale for image a is 10× the scale bar.

Table 1. Photophysical, Electrochemical, and Electronic Properties of Three Molecules and Their Thin Films

compds	solution absorption peak (nm) and intensity ($\times 10^5\ M^{-1}\ cm^{-1}$)	film absorption peak (nm) and intensity ($\times 10^4\ cm^{-1}$)	film absorption onset (nm)	film optical bandgap (eV)	HOMO (eV)	LUMO (eV)	electrochemical bandgap (eV)	hole mobility ($cm^2\ V^{-1}s^{-1}$)
ADPM	603, 0.62	627, 0.77	729	1.70	−5.38	−3.50	1.88	1.92×10^{-4}
BF2-ADPM	656, 1.66	693, 1.48	782	1.59	−5.68	−3.94	1.74	1.49×10^{-4}
BO-ADPM	724, 1.19	761, 0.76	845	1.47	−5.48	−4.02	1.46	1.57×10^{-4} (2.88×10^{-5})[a]

[a] Film processed with THF.

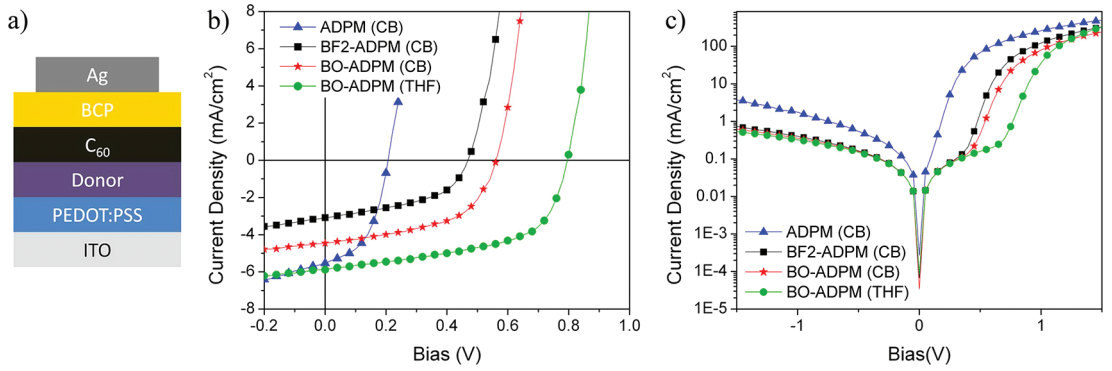

Figure 5. (a) Schematic device architecture and (b, c) the current density−voltage ($J-V$) characteristics of devices (b) under AM 1.5G simulated 1 sun solar illumination and (c) in the dark. CB denotes the use of chlorobenzene.

Table 2. Device Performance Characteristics for Planar Heterojunction Solar Cells with ADPM Donors

donor layer	thickness (nm)	V_{oc} (V)	J_{sc} (mA/cm^2)	FF	power conversion efficiency (%)	average power conversion efficiency (%)[a]
ADPM (CB)[b]	8.5	0.207	−5.53	0.487	0.56	0.54
BF2-ADPM (CB)	11.1	0.469	−3.088	0.475	0.69	0.66
BO-ADPM (CB)	12.3	0.562	−4.456	0.527	1.32	1.26
BO-ADPM (THF)	14.3	0.796	−5.882	0.562	2.63	2.53

[a] At least three devices were tested. [b] CB denotes chlorobenzene.

with root- mean-square(rms) roughness values of 0.29, 0.32, and 0.40 nm for BF2-ADPM from chlorobenzene, BO-ADPM from chlorobenzene, and BO-ADPM from THF, respectively. In contrast, ADPM forms large crystallites such that the surface is very rough with rms roughness of 5.7 nm.

Organic Solar Cells. Simple planar heterojunction solar cells were fabricated with the solution processed ADPM thin films as electron donors and vapor deposited C_{60} as the electron acceptor. As shown in Figure 5a, the resulting device structure was ITO/PEDOT:PSS(40 nm)/donor(8−15 nm)/C_{60} (45 nm)/BCP(10 nm)/Ag(100 nm).

We optimized the device performance by changing the solvents used and the solution concentrations for ADPM donor molecules. The solution processed donor layers were prepared via spin-casting solutions at 2000 rpm for 60 s, such that the film thickness was controlled by the solution concentration. We have obtained the best performing device with a power conversion efficiency of 2.63%, wherein the donor layer of ∼14 nm thick BO-ADPM was prepared from 2 mg/mL solution in THF. In addition, the best ADPM, BF2-ADPM, and BO-ADPM devices fabricated from cholorbenzene solutions showed power conversion efficiencies of 0.56, 0.69, and 1.32%, respectively. All devices were negatively affected by thermal annealing.

Figure 5b shows the current density vs voltage ($J-V$) curves for the four devices under AM 1.5G simulated solar illumination with an intensity of 100 mW cm^{-2}. The device characteristics are shown in Table 2. As far as the V_{oc} is concerned, the ADPM device exhibited the lowest value, which is consistent with its high HOMO level among the three compounds.[29] Additionally, the highly crystalline morphology of the ADPM film could result in strong molecular interactions between ADPM and C_{60} at the donor/acceptor interface, resulting in enhanced charge recombination.[18] Under conditions of high recombination, the forward bias current is high which results in a reduced V_{oc}. The dark current depends on the recombination in the device. Indeed, the highest dark current density for the ADPM device shown in Figure 5c supports our explanation. Compared to the ADPM device, the BF2-ADPM device exhibited a higher V_{oc} and lower J_{sc}, due to the much higher ΔE_{DA} and lower charge separation efficiency of BF2-ADPM/C_{60}.[29]

For the devices processed with cholorbenzene, the ADPM device showed much higher J_{sc} than the other two donors, although ADPM has the largest bandgap with lowest spectral overlap with solar irradiation. To gain a better understanding of the difference in J_{sc}, we measured the EQEs for the devices with different donor layers (Figure 6). The photocurrent generation for all devices is shown across a broad spectrum up to the near-infrared region, which matches well with the thin film absorption spectra as shown in Figure 2b. The low EQEs of ≤20% are very typical for planar heterojunction structured OSCs.[28] It was found that the ADPM/C_{60} device exhibited much higher EQE than the other donors. This is not surprising because ADPM/C_{60} has the highest energy offset between the LUMO levels of donor and acceptor, resulting in the highest charge separation efficiency. Additionally, the less flat molecular structure of ADPM could afford larger donor/acceptor distance in the bilayer interfaces leading to higher charge separation efficiency and subsequently higher J_{sc}.[34] It is worth mentioning that the EQE spectra past 800 nm were not measured because of limitations in our setup.

The BO-ADPM device is the most interesting with much higher performance than ADPM and BF2-ADPM devices. Also, the device characteristics show strong dependence on the processing solvent. Both the V_{oc} and J_{sc} increase significantly as a result of changing the processing solvent from cholorbenzene to THF. As demonstrated previously, a higher boiling point solvent would afford improved molecular stacking and

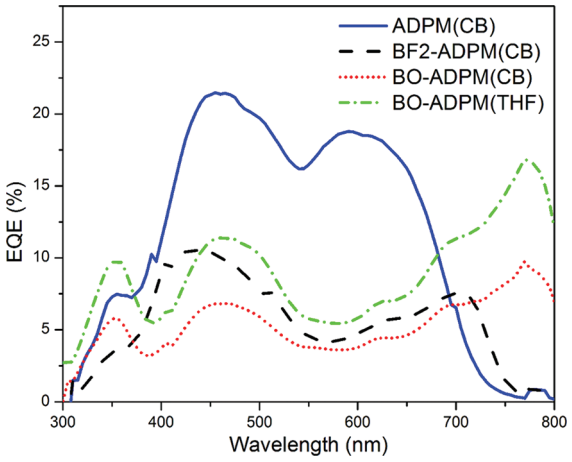

Figure 6. EQE spectra for ADPM donor-based devices. CB denotes chlorobenzene.

stronger molecule interactions after spin-casting.[30−33] In our case, stronger molecular interactions are believed to be present in the thin film processed by cholorbenzene with a boiling point of 131 °C than in the thin film processed by THF with boiling point of 66 °C. The increase in molecular interactions by processing with chlorobenzene is well-supported by an order of magnitude increase in the hole mobility compared to the mobility in films processed from THF. The increased alignment of BO-ADPM molecules in the cholorbenzene processed thin film could lead to stronger BO-ADPM/C_{60} interactions at the donor/acceptor interface, resulting in higher dark current, compared to processing from THF, as shown in Figure 5c. Ultimately, the BO-ADPM device with THF processed donor layer possesses weak donor/acceptor interaction, at the interfaces, low dark current, and subsequently high V_{oc},[18] as well as high charge transfer energy state allowing for high charge separation efficiency and subsequently high J_{sc}.[34] Our findings are consistent with observations in other molecular systems, and suggest that obtaining high J_{sc} and V_{oc} simultaneously is possible if we have good control of the thin film electronic and morphological properties.[18] More studies involving spectroscopic tools and theoretical calculations are underway to obtain an in-depth understanding of the correlations between the interfacial morphological/electronic properties and the device characteristics.

CONCLUSIONS

In conclusion, we have demonstrated efficient planar heterojunction organic solar cells with small molecular weight azadipyrromethens, a new family of solution-processable near-infrared donor materials with high extinction coefficients and broad spectral absorption into the near-infrared region. Of particular interest is a high open circuit voltage of ∼0.8 V that has been realized for the BO-ADPM/C_{60} devices with photocurrent generation up to 850 nm. A power conversion efficiency of 2.63% is among the highest values for planar heterojunction solar cells with solution processed near-infrared donor layers. Our work clearly shows the great potential of the application of ADPM-based molecules in OSCs. Ongoing research involves further improvement of the device performance with better control on the molecular electronic and morphological properties of these small molecules.

ASSOCIATED CONTENT

Supporting Information. Includes synthetic schemes for ADPM, BF2-ADPM, and BO-ADPM; 500 MHz ^{1}H NMR spectra of all three molecules; density functional theory calculated HOMO and LUMO surface plots; and cyclic voltammetry plots. This material is available free of charge via the Internet at http://pubs.acs.org.

AUTHOR INFORMATION

Corresponding Author
*E-mail: BWMa@lbl.gov.

ACKNOWLEDGMENT

This work was performed at the Molecular Foundry, Lawrence Berkeley National Laboratory, and was supported by the Office of Science, Office of Basic Energy Sciences, Scientific User Facilities Division, U.S. Department of Energy, under Contract DE-AC02—05CH11231. S.L. thanks University of California, Berkeley, for the Chancellor's Fellowship. L.C. thanks Department of Energy for the Science Undergraduate Laboratory Internships (SULI) program.

REFERENCES

(1) Forrest, S. R. *Nature* **2004**, *428*, 911–918.
(2) Hoppe, H.; Sariciftci, N. S. In *Photoresponsive Polymers II*; Marder, S. R.; Lee, K.-S., Eds.; Springer Berlin Heidelberg: Berlin, 2008; pp 1−86.
(3) Hoppe, H.; Sariciftci, N. *J. Mater. Res.* **2004**, *19*, 1924–1945.
(4) Lloyd, M. T.; Anthony, J. E.; Malliaras, G. G. *Mater. Today* **2007**, *10*, 34–41.
(5) Hains, A. W.; Liang, Z.; Woodhouse, M. A.; Gregg, B. A. *Chem. Rev.* **2010**, *110*, 6689–6735.
(6) Walker, B.; Kim, C.; Nguyen, T. -Q. *Chem. Mater.* **2011**, *23*, 470–482.
(7) Vasseur, K.; Rand, B. P.; Cheyns, D.; Froyen, L.; Heremans, P. *Chem. Mater.* **2011**, *23*, 886–895.
(8) Wang, W.; Placencia, D.; Armstrong, N. R. *Org. Electron.* **2011**, *12*, 383–393.
(9) Rand, B. P.; Xue, J.; Yang, F.; Forrest, S. R. *Appl. Phys. Lett.* **2005**, *87*, 233508.
(10) Ma, B.; Woo, C. H.; Miyamoto, Y.; Fréchet, J. M. J. *Chem. Mater.* **2009**, *21*, 1413–1417.
(11) Bürckstümmer, H.; Kronenberg, N. M.; Meerholz, K.; Wurthner, F. *Org. Lett.* **2010**, *12*, 3666–3669.
(12) Wei, G.; Wang, S.; Renshaw, K.; Thompson, M. E.; Forrest, S. R. *ACS Nano* **2010**, *4*, 1927–1934.
(13) Zhang, G.; Fu, Y.; Xie, Z.; Zhang, Q. *Macromolecules* **2011**, *44*, 1414–1420.
(14) Mei, J.; Graham, K. R.; Stalder, R.; Reynolds, J. R. *Org. Lett.* **2010**, *12*, 660–663.
(15) Kubo, Y.; Watanabe, K.; Nishiyabu, R.; Hata, R.; Murakami, A.; Shoda, T.; Ota, H. *Org. Lett.* **2011**, *13*, 4574–4577.
(16) Tamayo, A. B.; Walker, B.; Nguyen*, T.-Q. *J. Phys. Chem. C* **2008**, *112*, 11545–11551.
(17) Erwin, P.; Thompson, M. E. *Appl. Phys. Lett.* **2011**, *98*, 223305.
(18) Perez, M. D.; Borek, C.; Forrest, S. R.; Thompson, M. E. *J. Am. Chem. Soc.* **2009**, *131*, 9281–9286.
(19) Zhao, W.; Carreira, E. M. *Angew. Chem., Int. Ed.* **2005**, *44*, 1677–1679.
(20) Killoran, J.; O'Shea, D. F. *Chem. Commun.* **2006**, 1503.
(21) Hall, M. J.; Allen, L. T.; O'Shea, D. F. *Org. Biomol. Chem.* **2006**, *4*, 776.
(22) Gorman, A.; Killoran, J.; O'Shea, C.; Kenna, T.; Gallagher, W.; O'Shea, D. *J. Am. Chem. Soc.* **2004**, *126*, 10619–10631.

(23) Gallagher, W. M.; Allen, L. T.; O'Shea, C.; Kenna, T.; Hall, M.; Gorman, A.; Killoran, J.; O'Shea, D. F. *Br. J. Cancer* **2005**, *92*, 1702–1710.
(24) Loudet, A.; Bandichhor, R.; Burgess, K.; Palma, A.; McDonnell, S.; Hall, M.; O'Shea, D. *Org. Lett.* **2008**, *10*, 4771–4774.
(25) McDonnell, S. O.; O'Shea, D. F. *Org. Lett.* **2006**, *8*, 3493–3496.
(26) Ulrich, G.; Ziessel, R.; Harriman, A. *Angew. Chem., Int. Ed.* **2008**, *47*, 1184–1201.
(27) Hall, M. J.; McDonnell, S. O.; Killoran, J.; O'Shea, D. F. *J. Org. Chem.* **2005**, *70*, 5571–5578.
(28) Kekuda, D.; Huang, J.-H.; Ho, K.-C.; Chu, C.-W. *J. Phys. Chem. C* **2010**, *114*, 2764–2768.
(29) Brabec, C. J.; Cravino, A.; Meissner, D.; Sariciftci, N. S.; Fromherz, T.; Rispens, M. T.; Sanchez, L.; Hummelen, J. C. *Adv. Funct. Mater.* **2001**, *11*, 374–380.
(30) Li, G.; Shrotriya, V.; Huang, J.; Yao, Y.; Moriarty, T.; Emery, K.; Yang, Y. *Nat. Mater.* **2005**, *4*, 864–868.
(31) Park, S. K.; Jackson, T. N.; Anthony, J. E.; Mourey, D. A. *Appl. Phys. Lett.* **2007**, *91*, 063514.
(32) Chang, P. C.; Lee, J.; Huang, D.; Subramanian, V.; Murphy, A. R.; Fréchet, J. M. J. *Chem. Mater.* **2004**, *16*, 4783–4789.
(33) Chang, J.-F.; Sun, B.; Breiby, D. W.; Nielsen, M. M.; Sölling, T. I.; Giles, M.; McCulloch, I.; Sirringhaus, H. *Chem. Mater.* **2004**, *16*, 4772–4776.
(34) Holcombe, T. W.; Norton, J. E.; Rivnay, J.; Woo, C. H.; Goris, L.; Piliego, C.; Griffini, G.; Sellinger, A.; Brédas, J.-L.; Salleo, A.; Fréchet, J. M. J. *J. Am. Chem. Soc.* **2011**, *133*, 12106–12114.